H^0+H_2 and H^0+O_2 collisions at low kilo-electron-volt energies

E. J. Quintana and E. Pollack
Department of Physics, University of Connecticut, Storrs, Connecticut 06269-3046
(Received 13 May 1996)

Small-angle H^0+H_2 and H^0+O_2 collisions are studied at energies of 1.0, 2.0, and 3.0 keV. Time-of-flight techniques are used to identify the dominant direct scattering ($\rightarrow H^0$) processes. The stripping ($\rightarrow H^+$) and electron capture ($\rightarrow H^-$) channels are identified by electrostatic energy analysis. The probabilities and reduced differential cross sections for the dominant processes are determined as a function of $\tau\ (=E\theta)$, the reduced scattering angle. This is found to be a useful variable for plotting the probabilities and reduced cross sections for the processes studied, since the results at the different energies generally lie on common curves. The electronically inelastic processes are found to dominate the collision for $\tau>0.2$ keV deg in $H+H_2$ and $\tau>0.3$ keV deg in $H+O_2$. The stripping process in H_2 primarily results in $H^+ + H_2(X) + e^-$ while the $H^+ + O_2^-$ channel is found to dominate the small-angle stripping in O_2. [S1050-2947(96)09010-5]

PACS number(s): 34.50.Gb, 34.90.+q

I. INTRODUCTION

Studies of collisions involving low keV energy H^0 atoms with simple diatomic molecules can provide results that are of fundamental as well as practical importance. As an example, the H^0+H_2 case is of fundamental interest because it provides information on H_3. This is the simplest triatomic system to which approximation techniques can be applied for calculating the potential energy surfaces. Since the H_3 ground-state surface is repulsive, collision experiments present the most direct approach to test the calculations on this important surface. Collisions of low keV energy H^0 are particularly important at auroral altitudes. As an example, the collisional excitation of low keV energy H^0, to $H^0(2p)$ rather than electron capture by H^+, is the major source of Lyman α radiation in the hydrogen aurora [1]. As an additional example, H^0+O_2 cross-section data are required in modeling and interpreting the behavior of auroral and night airglow phenomena [2]. The low keV energy H^0 at auroral altitudes has its origin in a much higher energy H^+, which is incident on the upper atmosphere. The incident H^+ projectiles undergo inelastic collisions resulting in the excitation and ionization of the target atoms and molecules. The H^+ are primarily scattered through small angles in these collisions and degrade to energies where electron-capture processes become important. Electron capture then results in H^0 and H^- [1]. At auroral altitudes the H^0 component has a low keV energy distribution and is the dominant hydrogen projectile species.

To date H^0+H_2 collisions have primarily been studied at thermal energies, focusing therefore on atom-molecule chemical reactions. Valentini and Phillips [3] discussed the resurgence of interest in the H^0+H_2 dynamics following the availability of improved experimental results. There are, however, very few studies at higher energies that can directly probe the short-range part of the ground-state surface. This paper presents the results of measurements of the relative probabilities and relative reduced cross sections for the dominant collision processes at low keV energies. The results are particularly suited to provide some detailed information about the short-range part of the potentials and the coupling between energy surfaces. As in the atom-atom case, the electronically elastic differential results can best reveal the important features of the ground-state potential-energy surface.

In a recent paper [4] we presented results on the direct scattering, stripping, and electron capture in H^0+N_2. It was shown that the inelastic channels are dominant beyond the smallest scattering angles. As an example, at an energy of 1.0 keV they become more important than the elastic channel for scattering angles larger than 0.2°. In the present paper we report on H^0+H_2 and H^0+O_2 at energies of 1.0, 2.0, and 3.0 keV. We again find the elastic channels to be weak beyond the very smallest angles. Of particular interest is that the excitation probabilities and reduced cross sections for the various collision channels are found to scale reasonably well when plotted as a function of reduced scattering angle.

II. EXPERIMENTAL RESULTS: H^0+H_2 COLLISIONS

The experimental setup and techniques have previously been described [4,5] and are only outlined here. Briefly, an H^+ beam from a Colutron ion source is accelerated to the required energy (E). The beam is focused by an einzel lens and passes between two (0.5×0.5 cm) gold-plated electrodes, where a voltage pulsed at 0.3 MHz ''chops'' it for time-of-flight (TOF) energy-loss measurements. The beam is mass analyzed by a Wien filter and then passes through a charge-exchange cell filled with H_2. The residual H^+ component of the emerging beam is electrically deflected, leaving an H^0 beam which enters the scattering cell containing the target gas maintained at pressures for single collision conditions. The projectiles scatter through an angle θ and enter an electrostatic energy analyzer for energy-loss measurements on H^+ and H^-, which result from the collision. The H^0 passes undeflected through the analyzer to a time-of-flight (TOF) detector positioned 4.2 m from the scattering cell. The initial H^+ beam (prior to neutralization) has an energy full width at half maximum (FWHM) of 0.5 eV per keV and a FWHM angular spread of 0.1°. Following neutralization, the H^0 has a measured FWHM spread of 2.0 eV at 1.0 keV and a FWHM angular spread of 0.15°. Measure-

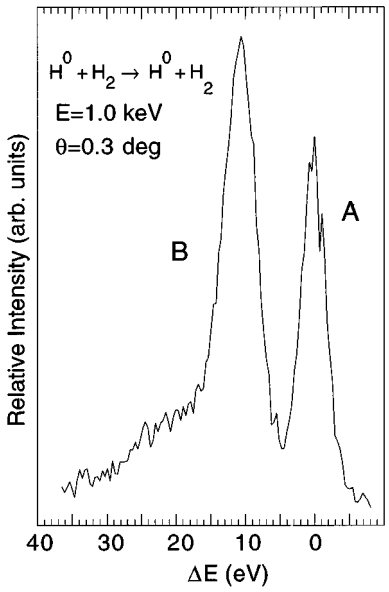

FIG. 1. Typical energy-loss spectrum for direct scattering of H^0 by H_2 at $E=1.0$ keV and $\theta=0.30°$. The two main peaks, 10.6 eV apart result from (A) electronically elastic collisions and (B) direct inelastic processes.

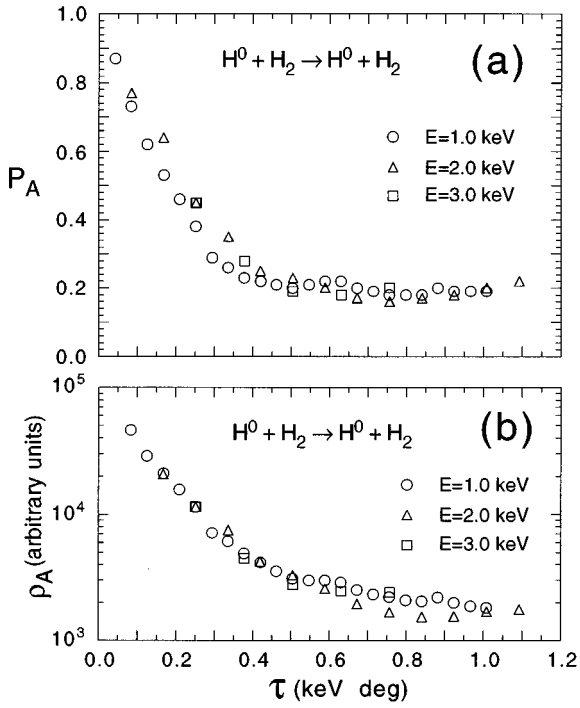

FIG. 2. (a) Probabilities for electronically elastic scattering (P_A) plotted as a function of reduced scattering angle, $\tau=E\theta$ for projectile energies $E=1.0$, 2.0, and 3.0 keV. The electronically inelastic processes are seen to dominate the scattering for $\tau>0.2$ keV deg. (b) The reduced differential cross section for elastic scattering, ρ_A $[=P_A\rho]$ as a function of τ. The results, at the three energies, are plotted to different arbitrary units and show that they can be approximated by a common curve in the angular range studied.

ments for the direct scattering ($\rightarrow H^0$), stripping ($\rightarrow H^+$), and electron capture ($\rightarrow H^-$) in H^0+H_2 collisions are made at energies of 1.0, 2.0, and 3.0 keV and at angles $0.05°<\theta<1.0°$. The energy-loss spectra found in H^0+H_2 collisions show a number of peaks that correspond to the dominant exit channels of the collision. The identification of these final states is made using the potential-energy curves for the H_2 molecule [6]. Electronic excitations are assumed to result from vertical transitions occurring within the Franck-Condon (FC) region of the $H_2(X\ ^1\Sigma_g^+,\ \nu=0)$ potential-energy curve.

A typical spectrum for the direct scattering in H^0+H_2 is shown in Fig. 1. Peak A, at an energy loss $\Delta E=0$ eV, corresponds to the electronically elastic channel. Peak B is attributed to one-electron excitation of either the H_2 target or the H^0 projectile. An excitation of H_2 ($B\ ^1\Sigma_u^+$) from the H_2 ground state has a threshold energy-loss $\Delta E\approx11.5$ eV. Excitation of the projectile to the H^0 ($n=2$) state has $\Delta E\approx10.2$ eV. Contributions from these two channels most probably result in the peak B maximum at a measured $\Delta E=10.6$ eV. The small bump for $18<\Delta E<27$ eV observed primarily at larger τ (the reduced scattering angle$=E\theta$) values is attributed to two electron excitations. These may include $H^*+H_2^*$ as well as excitation of doubly excited states of the target H_2 molecule [7]. The H_2 ($b\ ^3\Sigma_u^+$) state, which dissociates into two ground state hydrogen atoms, is not noticeably excited.

The probability for the excitation of a particular exit channel in the collision is obtained at a given angle by taking the ratio of the relevant peak area to the total area of the entire spectrum. Figure 2(a) shows P_A, the probability for electronically elastic scattering, as a function of τ. In this plot, which emphasizes general features common to the collision energies in the experiment, it is seen that a single curve can be drawn through the results for the different energies studied. P_A decreases quite rapidly and drops below 0.5 for $\tau>0.2$ keV deg.

At each energy, the measured angular distributions of the scattered projectiles provide a ''summed'' differential cross section (SDCS) and ρ, a ''summed'' reduced differential cross section $[=\theta^2\times$(SDCS) at small angles]. These cross sections refer to all the projectiles in a given charge state, which are scattered at angle θ. Hence, the SDCS for $H^0+H_2\rightarrow H^0$ includes contributions from the elastic scattering as well as from the direct inelastic processes. Similar measurements, of the SDCS, for the direct scattering of H^0 by H_2, performed without energy analysis were reported by Johnson *et al.* [8]. Their results provided absolute summed differential cross sections at 0.5, 1.5, and 5.0 keV for scattering angles in the range of 0.05° to 0.5°. The absence of results at common energies in our studies precludes any quantitative comparison of the two experiments. However, the general qualitative features are seen to be in agreement in the angular range common to both studies.

The reduced cross section for a given channel is found by multiplying the ''summed'' ρ by the corresponding excitation probability. Figure 2(b) presents the ρ_A vs τ plot for electronically elastic scattering, which corresponds to peak A in the direct scattering spectrum. The results for the three energies are normalized to show the common general behavior at the beam energies investigated. It can be seen that ρ_A, which can be approximated by a single curve, decreases smoothly with increasing τ value.

In addition to the direct elastic and inelastic collisions, charge-changing processes are excited in keV energy H^0+H_2 collisions [9,10]. In these collisions simultaneous excitation

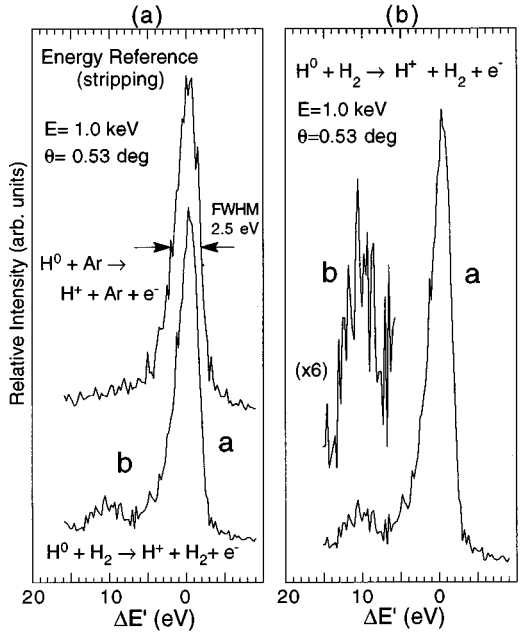

FIG. 3. (a) Energy reference for stripping collisions is provided by composite spectra from H^0+Ar and H^0+H_2 collisions. The main peaks (labeled a) are attributed to the $H^0+Ar \rightarrow H^+ + Ar + e^-$ reference and to $H^0+H_2 \rightarrow H^+ + H_2(X) + e^-$. These are seen to basically have the same excitation energy ($\Delta E = \Delta E' + 13.6$ eV) and shape (FWHM$\approx$2.5 eV). (b) The energy loss spectrum for stripping in H^0+H_2 collisions includes two peaks separated by 10.0 eV and attributed to stripping with H_2 remaining in its ground state (peak a) and stripping with simultaneous excitation of the H_2 target (peak b).

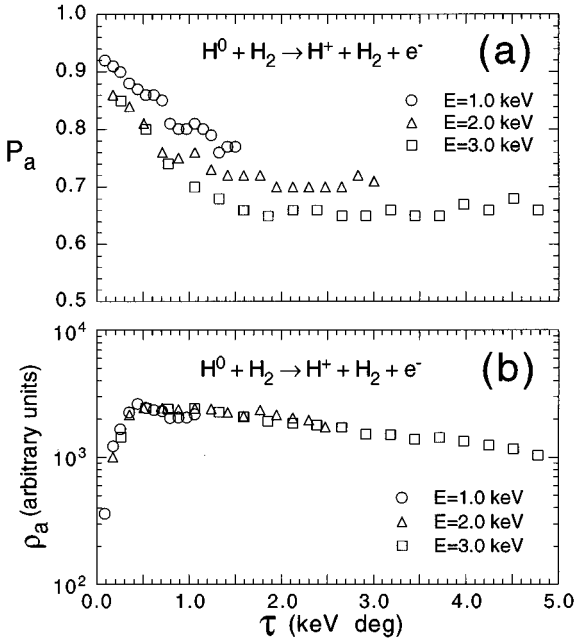

FIG. 4. (a) Probability for stripping with the H_2 target remaining in its ground state (P_a) is shown as a function of reduced scattering angle τ. (b) The reduced cross section, ρ_a, for stripping with the resulting H_2 target in the ground state as a function of τ. The normalized ρ_a vs τ results are well approximated by a curve common to the incident beam energies.

of the resulting molecular target is also found. Since the incident and detected beams are in different charge states, the energy losses of the scattered product ions must be established by using an energy spectrum from a known collision process. In this study $H^0+Ar \rightarrow H^+/H^-$ collisions provide the reference energies. Figure 3(a) shows composite spectra for $H^0+Ar \rightarrow H^+ + Ar + e^-$ and $H^0+H_2 \rightarrow H^+ + H_2 + e^-$ collisions. These spectra, for stripping collisions, are taken by rapidly switching the target gas. In both spectra the main peaks have the same basic shape (FWHM$\approx$2.5 eV) and location. This shows that they result primarily from the stripping of the projectile electron with the target remaining in the ground state. The stripping requires a minimum energy loss $\Delta E = 13.6$ eV. In the spectra for $H^0+H_2 \rightarrow H^+$, the reported energy losses ($\Delta E'$) are measured relative to stripping peak a, which is positioned at $\Delta E' = 0.0$ eV but has an excitation energy $\Delta E = 13.6$ eV. The actual energy loss for a particular stripping peak is given by $\Delta E = \Delta E' + 13.6$ eV. The broadening observed toward larger energy loss can be attributed to the excess kinetic energy carried off the ejected electron. The spectrum in Fig. 3(b) shows a magnification of the small peak labeled b which involves stripping with simultaneous excitation of the target, $H^0+H_2 \rightarrow H^+ - H_2^* + e^-$. The two-electron excitation processes found at $8 < \Delta E' < 13$ eV with an approximate maximum at $\Delta E' = 10.5$ eV have absolute energy losses $21.6 < \Delta E < 26.6$ eV. The $H^0+H_2 \rightarrow H^+ + H_2^-$ channel with a slightly larger energy loss ($\Delta E' = 2.0$ eV on the spectrum) than $H^0+H_2 \rightarrow H^+ + H_2 + e^-$ is not readily noticeable.

The probability, P_a, for electron stripping from the H^0 with the target H_2 molecule left in the ground state is shown in Fig. 4(a). A slight energy dependence can be noted in the probability as a function of τ. The corresponding ρ_a vs τ plot for stripping with the H_2 target remaining in its ground state, shown in Fig. 4(b) is obtained by multiplying the ρ for $H^0+H_2 \rightarrow H^+$ with P_a. The results for the three energies are normalized to show that the reduced cross sections scale reasonably well in the angular range studied.

The electron capture is generally much weaker than the two processes already discussed. Certain electron-capture processes are found to have energy losses comparable to those in the direct scattering and projectile stripping collisions. The energy reference spectra in Fig. 5(a) show peaks from $H^0+H_2 \rightarrow H^-(1s^2)+Ar^+$ and $H^0+H_2 \rightarrow H^-$. Since the polarity of the voltage applied to the back plate of the electrostatic energy analyzer is different for H^+ and H^- measurements, the $H^0+H_2 \rightarrow H^-$ energy-loss scale ($\Delta E'$) is reversed here. The ionization potentials of Ar and H_2 are less than one third of an eV apart and since the main peaks are at approximately the same location the peak labeled α can be attributed to $H^0+H_2 \rightarrow H^-(1s^2)+H_2^+(X)$. The energy losses are measured from the maximum of peak α (set at $\Delta E' = 0.0$ eV). Hence, the actual energy losses for the electron-capture processes are $\Delta E = \Delta E' + 14.8$ eV. Figure 5(b) shows the spectrum at $E = 2.0$ keV, which consists primarily of two main peaks separated by $\Delta E' = 9.6$ eV. Although the energy losses seen in peak β (8 eV$< \Delta E' <$14 eV) are consistent with electron capture to excited states of H^-, these states are not expected to live long enough to reach the detector. The singly excited levels, $H^-(1s2s)$ at $\Delta E' \approx 2.49$ eV and $H^-(1s2p)$ $\Delta E' \approx 3.11$ eV have been extensively discussed in astro-

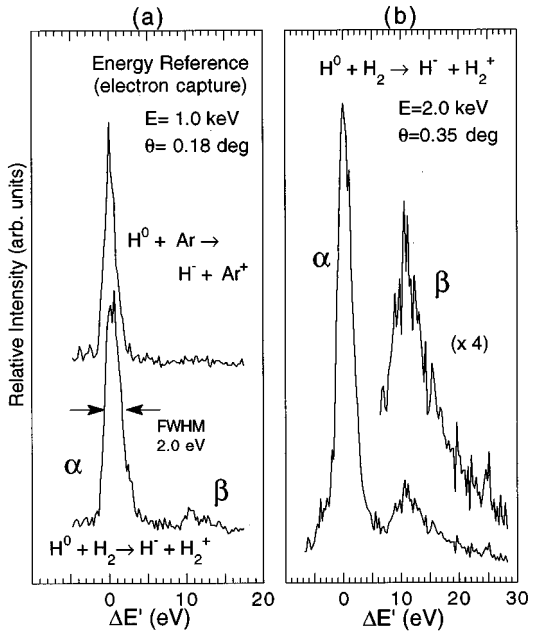

FIG. 5. (a) Using $H^0+Ar \rightarrow H^- (1s^2)+Ar^+$ collisions as an energy reference, peak α corresponds to $H^0+H_2 \rightarrow H^-(1s^2)+H_2^+(X)$ with an excitation energy $\Delta E=\Delta E'+14.8$ eV. (b) The two main peaks (α and β) for electron capture in H^0+H_2 collisions are separated by 9.6 eV. Peak β is consistent with a number of possible electronic excitations of the H^- or H_2^+. In electron-capture spectra the energy-loss scale is reversed since the detected beam is negatively charged.

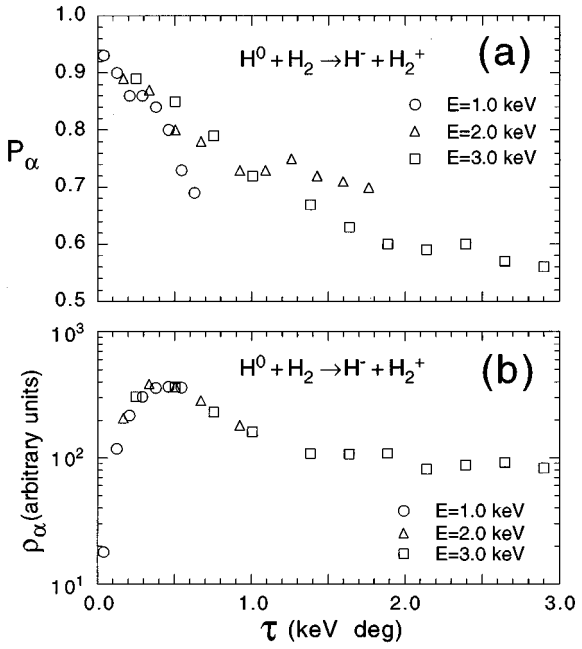

FIG. 6. (a) Probability (P_α) for $H^0+H_2 \rightarrow H^-(1s^2)+H_2^+(X)$ as a function of τ. At the larger τ values, P_α is seen to level off to approximately 0.5. (b) The corresponding normalized reduced cross sections (ρ_α) for $H^0+H_2 \rightarrow H^-(1s^2)+H_2^+(X)$ are seen to scale reasonably well in the angular range studied.

physical studies [11] but have not been observed in the laboratory. The autodetaching states H^- ($n=2$) at $\Delta E' \approx 10.5$ eV and H^- ($n=3$) at $\Delta E' \approx 12.5$ eV which have been identified in electron spectra for H^- scattering experiments [12] are however, too short-lived ($\approx 10^{-11}$ to 10^{-14} sec.) to contribute to the spectra at the observed energy losses. There has been speculation about some doubly excited H^- states for which parity in the e-e interaction does not allow decay to the H^- ground state by autodetachment [13]. Such excitations may survive long enough to be seen in the energy-loss spectra for electron capture.

Figure 6(a) shows P_α, the probability for electron capture to ''channel'' α, as a function of τ. This process involving projectile electron capture to $H^-(1s^2)+H_2^+(X\ ^2\Sigma_g^+)$ is seen to dominate in the angular range investigated. The collision mechanism involved here is the simple transfer of a single electron from one ''center'' to another. Figure 6(b) is a plot of ρ_α, the reduced differential cross section for the electron capture, as a function of τ. The results at the three energies are normalized and are seen to scale reasonably well in the angular range investigated.

III EXPERIMENTAL RESULTS: H^0+O_2 COLLISIONS

An energy-loss spectrum for the direct scattering in H^0+O_2 collisions, at $E=1.0$ keV and $\theta=0.36°$, is shown in Fig. 7. Peak A corresponds primarily to electronically elastic scattering. This peak, having a FWHM=2.4 eV, may also include weak excitation of the singlet $O_2(a\ ^1\Delta_g)$ and $O_2(b\ ^1\Sigma_g^+)$ states. Electronically inelastic processes, which include single-electron excitations of the O_2 target molecule, excitation of the projectile to the $H^0(n=2)$ state, and simultaneous projectile and target excitations are labeled B. Its distinct features can be observed only in some spectra at the smaller scattering angles ($\theta<0.4°$). The structure at $\Delta E \approx 5.4$ eV can be associated with excitation of any one in a group of O_2^* states ($C\ ^3\Delta_u$, $A\ ^3\Sigma_u^+$, $c\ ^1\Sigma_u^-$). At $\Delta E \approx 8.5$ eV $O_2^*(B\ ^3\Sigma_u^-)$ and at $\Delta E \approx 10.9$ eV the $O_2^*(^1\Delta_u)$, $O_2^*(^1\Sigma_u^+)$ and $H^0(n=2)$ may contribute. The broad structure in the

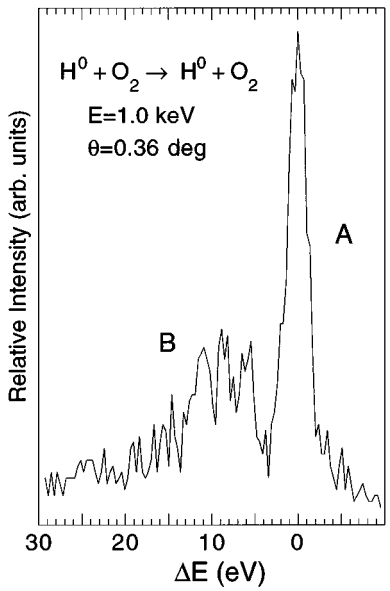

FIG. 7. Typical energy-loss spectrum for direct scattering in H^0+O_2 at $E=1.0$ keV and $\theta=0.36°$. The peak labeled A corresponds primarily to electronically elastic scattering. The structure labeled B is due to electronically inelastic processes.

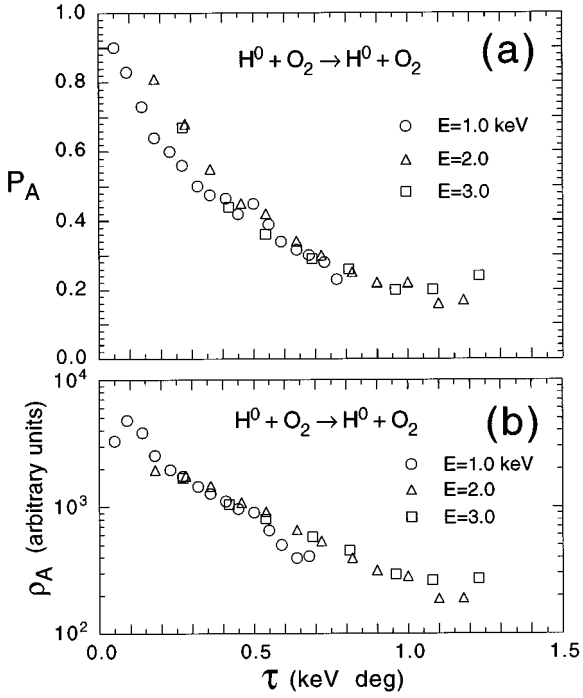

FIG. 8. (a) Probability for electronically elastic scattering (P_A) in H^0+O_2 as a function of reduced scattering angle. The direct inelastic processes are seen to be dominant for $\tau>0.3$ keV deg. (b) The reduced cross section (ρ_A) as a function of reduced scattering angle for electronically elastic scattering in H^0+O_2 collisions. The results are normalized to show that they can be approximated by a common curve for the three beam energies.

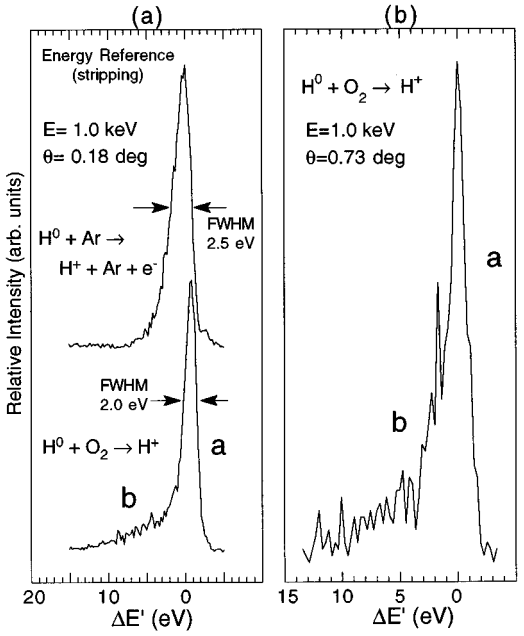

FIG. 9. (a) Energy reference for stripping in H^0+O_2 collisions. In the composite spectra the reference peak corresponding to $H^0+Ar \rightarrow H^+ + Ar + e^-$ is separated by an energy loss of about 0.8 eV from the peak attributed to $H^0+O_2 \rightarrow H^+ + O_2^-(X)$. The narrower peak shape for $H^0+O_2 \rightarrow H^+$, FWHM$\sim$2.0 eV, further indicates that the primary stripping channel involves electron capture by the target rather than loss to the continuum. (b) A typical energy-loss spectrum for stripping in H^0+O_2 collisions shows a main peak (a) attributed to the $H^+ + O_2^-(X\ ^2\Pi_g)$ channel. There is additional structure (b) corresponding to stripping with simultaneous excitation of the O_2 target.

range $13.6<\Delta E<20$ eV is attributed to simultaneous excitation of the O_2 and H^0 projectile. The electronic excitation processes associated with features in the energy-loss spectra are identified using the O_2 potential-energy curves of Gilmore [14]. These curves have to be extrapolated when considering ''vertical'' transitions in the FC region of the $O_2(X\ ^3\Sigma_g^-,\ \nu=0)$ ground-state curve. In most instances, the transitions near the outer turning point of the O_2 ground-state curve ($R=1.27$ Å) provides the threshold value of the excitation energy for our state identifications.

The probability for electronically elastic scattering (P_A) is presented in Fig. 8(a) as a function of τ. The electronically inelastic processes are seen to be dominant for $\tau>0.3$ keV deg. At $\tau=1.0$ keV deg, electronically inelastic processes account for as much as 80% of the direct scattering channel. The reduced differential cross section (ρ_A) for $H^0(1s)+O_2(X) \rightarrow H^0(1s)+O_2(X)$ is shown in Fig. 8(b). The normalized plots at the three energies are again seen to exhibit common general features except at the smallest scattering angles.

The energy reference for stripping collisions, shown in Fig. 9(a), is obtained from $H^0+Ar \rightarrow H^+$. The main peaks for the Ar and O_2 targets are separated by a $\Delta E'\approx 0.8$ eV showing that peak a in the O_2 case corresponds to $H^+ + O_2^-(X\ ^2\Pi_g)$. The narrower peak shape for $H^0+O_2 \rightarrow H^+$, with a FWHM$\approx$2.0 eV provides further confirmation for electron capture by the target rather than loss to the continuum. The structure at the higher energy-loss side of peak a is consistent with stripping (to the continuum) and the simultaneous excitation of the singlet O_2 ($a\ ^1\Delta_g$) and O_2 ($b\ ^1\Sigma_g^+$) states.

These excitations at $\Delta E'\approx 1.7$ eV are more apparent in the spectrum, in Fig. 9(b), at $E=1.0$ keV and $\theta=0.73°$. Additional structure seen at energy losses $4.2<\Delta E'<11.0$ eV are consistent with excitation of the same O_2* states ($C\ ^3\Delta_u$, $A\ ^3\Sigma_u^+$, $c\ ^1\Sigma_u^-$, $B\ ^3\Sigma_u^-$, and $^1\Delta_u$) that contribute to the direct inelastic scattering. As in the spectra for stripping in H^0+H_2 collisions, the energy-loss differences, $\Delta E'$, are shown relative to the maximum of the peak which is labelled a and positioned at $\Delta E'=0.0$ eV. The absolute energy losses are given by $\Delta E=\Delta E'+13.1$ eV.

Figure 10(a) shows P_a, the probability of exciting $H^+ + O_2^-(X\ ^1\Pi_g)$ in a stripping collision, as a function of τ. Weak contributions from electron loss to the continuum $H^0+O_2 \rightarrow H^+ + O_2(X) + e^-$ cannot be ruled out, however. The corresponding normalized reduced differential cross sections (ρ_a) shown as a function of τ in Fig. 10(b) are seen to scale well for the three energies studied.

Projectile electron capture in H^0+O_2 collisions involves the transfer of an electron from the molecular target to the projectile requiring an energy loss of at least 11.8 eV. Figure 11(a) shows the main peaks for the $H^0+Ar \rightarrow H^-(1s^2)+Ar^+$ energy reference spectrum and for $H^0+O_2 \rightarrow H^-$. The peaks are separated by 3.35 eV indicating that this electron capture from O_2 leaves the resulting product ions in their ground electronic states. The similar peak shapes (FWHM$\approx$2.0 eV) for both the O_2 and Ar cases further supports this assignment. In the spectrum at $E=3.0$ keV and $\theta=0.27°$ shown in Fig. 11(b) $\Delta E'$, the energy losses are measured from peak α

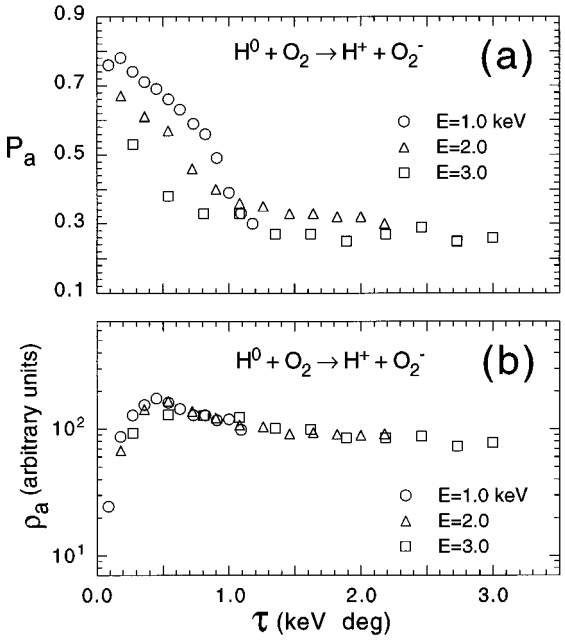

FIG. 10. (a) Probability (P_a), for stripping primarily to $H^+ + O_2^-(X\ ^1\Pi_g)$, as a function of τ. (b) The corresponding reduced cross section (ρ_a) as a function of τ. The normalized results for ρ_a can be approximately fitted by a common curve at the three collision energies studied.

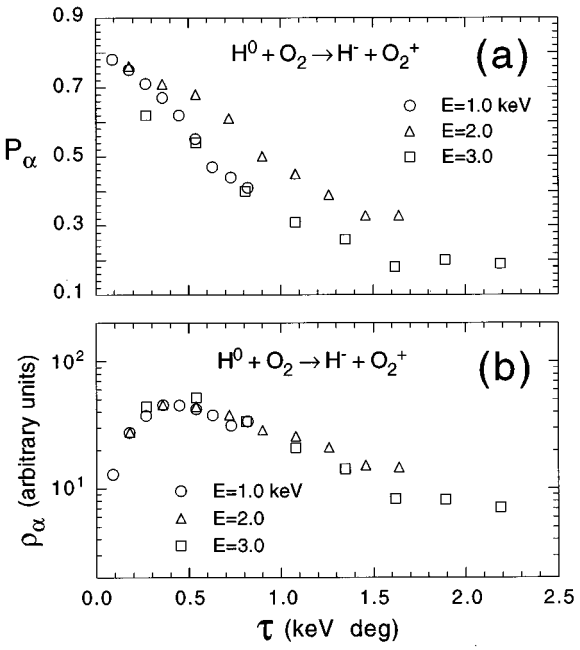

FIG. 12. (a) Probability (P_α) for projectile electron capture to the ground state in H^0+O_2 collisions as a function of τ. (b) The corresponding normalized reduced cross sections as a function of τ are seen to be reasonably well fitted by a curve common to the three energies studied.

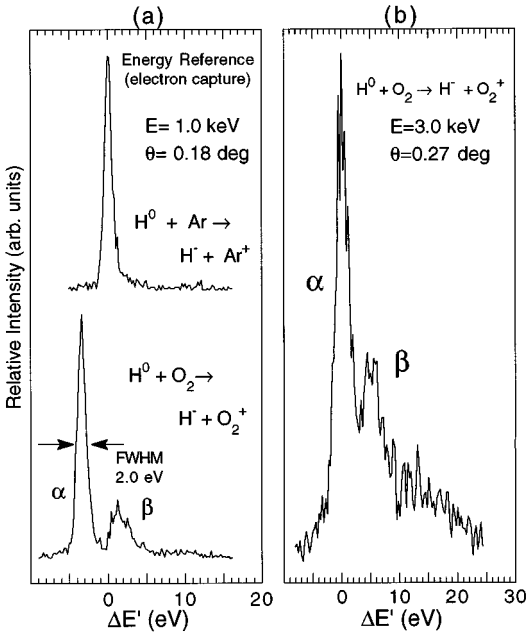

FIG. 11. (a) Energy reference for electron capture in H^0+O_2 collisions is provided by the known collision process, $H^0+Ar \rightarrow H^-(1s^2)+Ar^+$. The main peaks in the composite spectra are separated by an energy difference of 3.35 eV showing that peak α corresponds to $H^0+O_2 \rightarrow H^-(1s^2)+O_2^+(X\ ^2\Pi_g)$. (b) The energy-loss spectrum for electron capture in H^0+O_2 collisions involve two main peaks separated by 4.8 eV. The peak labeled β is attributed primarily to $H^0+O_2 \rightarrow H^-(1s^2)+O_2^+(A\ ^2\Pi_u)$, $H^0+O_2 \rightarrow H^-(1s^2)+O_2^+(a\ ^4\Pi_u)$ and $H^0+O_2 \rightarrow H^-(1s^2)+O_2^+(b\ ^2\Sigma_g^-)$.

which corresponds primarily to $H^0+O_2 \rightarrow H^-(1s^2)+O_2^+(X\ ^2\Pi_g)$. For electron capture in H^0+O_2 the absolute energy losses are given by $\Delta E = \Delta E' + 11.8$ eV. Peak β with its maximum at $\Delta E' \approx 4.8$ eV is consistent with $H^0+O_2 \rightarrow H^-(1s^2)+O_2^+(A\ ^2\Pi_u)$ and the structure at $\Delta E' \approx 6.0$ eV with $H^0+O_2 \rightarrow H^-(1s^2)+O_2^+(b\ ^4\Sigma_g^-)$. Other exit channels involving possible electron capture to the singly excited $H^-(1s2s)/(1s2p)$ and $O_2^+(a\ ^4\Pi_u)/(B\ ^2\Sigma_g^-)$ also fall within peak β's energy-loss range $2.5 < \Delta E' < 9.5$ eV. The structure at $10 < \Delta E' < 19$ eV, which is not noticeable at $E = 1.0$ keV, is more apparent in the $E = 3.0$ keV spectrum. Excitations corresponding to these energy-loss differences involve higher lying O_2^+ states and possibly doubly excited states of H^-, which live long enough to reach the detector.

The probability (P_α), for exciting $H^0+O_2 \rightarrow H^-(1s^2)+O_2^+(X\ ^2\Pi_g)$ in an electron-capture collision, and the corresponding reduced cross section (ρ_α) are plotted as functions of τ in Figs. 12(a) and 12(b). The normalized results show that ρ_α can again be fit by a curve common to the three energies studied.

IV. CONCLUSIONS

The direct scattering results obtained in H^0 collisions with H_2 and O_2 are very similar to those found in our earlier study on N_2 [4]. In low keV energy atom-atom and atom-molecule collisions the elastic channels generally dominate the scattering at small angles. In sharp contrast, our studies on H^0+H_2, O_2, and N_2 show that the inelastic channels dominate in these collisions beyond the smallest angles ($\tau > 0.2$, 0.3, and 0.2 keV deg respectively). In a paper on charge production in H^0+N_2, Van Zyl *et al.* [15] suggested that ionic states play

an important role in the collision. Our studies support the role of intermediate ionic channels in the direct scattering. As an example, at infinite separation the lowest $H^-+H_2^+$ ionic state lies about 15 eV above the incident H_3 potential energy surface. As the interparticle separation decreases during the collision, the attractive ionic curve crosses the repulsive incident surface. The ionic channels excited at these crossings can then couple to the observed $H+H_2$* and H^*+H_2 channels since they lie close in energy to them at large interparticle separation. The dominance of inelastic collisions at small angles supports this model of the collision since the intermediate ionic states are attractive and result in a decreased scattering angle. Our work also shows that the reduced scattering angle (related to the distance of closest approach during a collision), is a generally useful variable for plotting experimental results. Several aspects of our H^0+O_2 study are of particular interest. The direct scattering in these collisions is shown to excite dissociating O_2 states which result in atomic oxygen. In addition the small angle stripping to H^+ is dominated by the capture of the electron to bound O_2^- which does not contribute to the production free electrons. These results show than an understanding of the H^0+O_2 collision is important in modeling atmospheric processes.

ACKNOWLEDGMENTS

This work was supported by the Connecticut Space Grant College Consortium under NASA Grant No. NGT-40037 and the University of Connecticut Research Foundation. We wish to thank Dr. Valerie Heckman for her contributions to the research.

[1] R. J. McNeal and J. H. Birely, Rev. Geophys. Space Phys. **11**, 663 (1973).
[2] J. F. Noxon, J. Geophys. Res. **75**, 1879 (1970).
[3] J. J. Valentini and D. L. Phillips, in *Bimolecular Collisions*, edited by M. N. R. Ashfold and J. E. Baggott (Royal Soc. of Chemistry, London, 1989), p.1.
[4] E. J. Quintana and E. Pollack, Phys. Rev. A **53**, 206 (1996).
[5] E. Pollack and Y. Hahn, Adv. At. Mol. Phys. **22**, 243 (1986).
[6] T. E. Sharp, At. Data **2**, 119 (1971).
[7] S. L. Guberman, J. Chem. Phys. **78**, 1404 (1983).
[8] L. K. Johnson, R. S. Gao, K. A. Smith, and R. F. Stebbings, Phys. Rev. A **38**, 2794 (1988).
[9] G. J. Smith, L. K. Johnson, R. S. Gao, K. A. Smith, and R. F. Stebbings, Phys. Rev. A **44**, 5647 (1991).
[10] M. W. Gealy and B. Van Zyl, Phys. Rev. A **36**, 3100 (1987).
[11] C. Ingemann-Hilberg and M. Rudkjobing, Astrophys. Space Sci. **6**, 101 (1970).
[12] J. S. Risley, A. K. Edwards, and R. Geballe, Phys. Rev. A **9**, 115 (1974).
[13] G. W. F. Drake, Phys. Rev. Lett. **24**, 126 (1970).
[14] F. R. Gilmore, J. Quant. Spectrosc. Radiat. Trans. **5**, 369 (1965).
[15] B. Van Zyl, H. Neumann, T. Q. Le, and R. C. Amme, Phys. Rev. A **18**, 506 (1978).